Cranking inertia of odd nuclei from time-dependent pairing equations: Application to Th cold fission

M. Mirea*

Horia Hulubei National Institute for Physics and Nuclear Engineering, P.O. Box MG-6, 077125 Bucharest-Magurele, Romania and Academy of Romanian Scientists, Splaiul Independentei 54, 050094 Bucharest, Romania

(Received 18 April 2019; revised manuscript received 4 June 2019; published 17 July 2019)

A new formalism for the nonadiabatic collective inertia from time-dependent pairing equations for odd numbers of nucleons is described in detail. The effective masses and the moments of inertia result from the occurrence of matrix elements of the time derivatives and of the angular couplings, respectively, between states of different seniority configurations. For low collective velocities, the formulas for the inertia reduce to the known cranking expressions available for quasitationary states. The effective mass and the perpendicular moment of inertia are evaluated for the $^{230-232}$Th parent nuclei along the fission path. The inertia for the even-odd system is larger than those of the even-even ones and exhibits fluctuations due to the intrinsic nuclear structure. The ground state theoretical value of the moment of inertia for ^{231}Th agrees well with the evaluated experimental data if the blocking effect is neglected.

DOI: 10.1103/PhysRevC.100.014607

I. INTRODUCTION

In treatments of nuclear reactions, it is usually considered that the nucleons move in an average deformed field managed by some external constraints. These external constraints can be the shape collective coordinates associated with some degrees of freedom or the angles between the intrinsic coordinate system and the laboratory one. Quantities such as moments of inertia and effective masses are defined in terms of these collective coordinates. The vibrational and rotational motions of the collective parameters modify the average field. In the original cranking model [1–4], it is assumed that the collective parameters vary slowly in time, thus allowing the nucleons to follow in an adiabatic way the average field. By considering instantaneous values of the collective velocities and by preserving the total energy of the nuclear system, formulas for the collective moments of inertia and of the effective inertia are deduced. That is, the original derivations of the cranking theories are treated in the lowest order perturbation of the collective velocity. A generalization was provided by constructing a self-consistent potential that takes into account the influence of the collective velocities [5], leading to the cranked model. Different approaches were developed to improve the calculation of the inertia in this direction. For example, a prescription that gives all order corrections in powers of an inverse timescale is presented Ref. [6]. A cranking inertia that takes into account the collective velocity dependence of the potential and of the pairing field was developed in Ref. [7]. The dependence of the cranking parameters on the internal excitation was also investigated [8–12]. But, the most important development of the cranking formalism is the consideration of the residual interactions in calculations. With the inclusion of pairing [13,14], moments of inertia were evaluated realistically for the first time in Refs. [15,16]. The cranking superfluid model reported a remarkable success in describing the values of the moments of inertia [17–25] of even-even nuclei in their ground states and in their isomeric states. Superfluid systems mean that the fluid inertia is strongly suppressed. In self-consistent approaches, a cranking operator or perturbative approach is used to determine the inertia corresponding to an adiabatic motion [26–36].

The original derivation of the moments of inertia for odd-nuclei is based on Green functions [37]. A first investigation of the odd-nuclei configurations was realized in Ref. [38] without treating explicitly the blocking effect. Many other contributions were also developed over time in Refs. [39–45] aiming to achieve a better accuracy of the approach. By investigating explicitly the influence of the blocking effect [43] which occurs when the excitations change the seniority by 2 units, it was confirmed that the moments of inertia of odd-A nuclei are larger than those of both neighboring even-even nuclei. It was also estimated in Ref. [46] that the moment of inertia increases typically by about 15% if the squared pairing gap is halved. Such an effect can be produced by the reduction of the pair correlations due to the presence of the unpaired particle. The Coriolis couplings between the lowest one-quasiparticle state and the remaining one-quasiparticle states cause more important variations of the inertia. It is important to note that both contributions are strongly influenced by the specific microscopic nuclear structure. Surprisingly, reduced moments of inertia due to the presence of the odd particle [47] were obtained for certain intrinsic configurations.

In the following, I use a new formalism intended to obtain on the same footing the radial and the rotational inertia for systems with an odd number of nucleons. This non-adiabatic

*mirea@ifin.nipne.ro

treatment is derived from the time-dependent pairing equations and it is described in detail, following the main lines proposed in Refs. [48,49] for even nuclei. The inertia emerges as a response of the nuclear system to infinitesimal changes of the collective coordinates under the action of external forces, with the generalized velocities being unchanged. Concomitantly, the time-dependent pairing equations are also obtained by appealing to the variational principle applied to the same functional. That gives the possibility to calculate the dissipated energy when the collective coordinates change in time. Therefore, the mass parameters obtained within the proposed recipe depend also on the dissipated energy.

An evaluation of the dissipated energy is given by the difference between the many-body energy obtained by solving the time-dependent pairing equations and the many-body energy calculated adiabatically at the same collective deformation. As discussed in Ref. [50], this calculation is completely reversible. If all the coordinates are time reversed, the nuclear system retraces its path. That means a part of the collective kinetic energy is stored temporarily in the microscopic degrees of freedom as a conservative potential, allowing the system to oscillate with small amplitudes around its equilibrium. For a large amplitude motion, the elongation can exceed the scission point. When the two fission fragments are stopped in some detectors, this part of the collective kinetic energy stored temporarily is transferred irreversibly in intrinsic excitation. Such an event can be called randomization and, as suggested in Ref. [50], a major part of the above defined dissipated energy can be interpreted as being irreversible from the macroscopic point of view.

In this work, I consider low velocities, therefore the influences of the collective velocities on the single-particle states are disregarded. For these velocities the nuclear system behaves adiabatically, the dissipated energy is negligible, and the BCS solutions of the microscopic equations of motion follow accurately the values obtained for quasitationary states [51]. The mean field is obtained within the Woods-Saxon two-center shell model [52].

As an application, the fission of Th isotopes at low energies is analyzed along the fission path, starting from the ground state, overcoming the exit point of the barrier and reaching the final two fragments configuration. The behavior of the inertia is investigated for such a large scale amplitude motion in adiabatic conditions.

II. DERIVATION OF THE COLLECTIVE INERTIA

In this section, the inertia formalism is described. By appealing to the variational principle, the moments of inertia and the effective masses are deduced. The functional

$$\mathcal{L} = \langle\varphi|H - i\hbar\frac{\partial}{\partial t} - \vec{\Omega}\vec{J} - \lambda\hat{N}|\varphi\rangle, \tag{1}$$

is constrained by two Lagrange multipliers, λ and Ω. In the previous expression, H denotes the independent single-particle Hamiltonian with pairing residual interactions:

$$H = \sum_l \epsilon_l(a_l^+ a_l + a_{\bar{l}}^+ a_{\bar{l}}) - G\sum_n\sum_l a_n^+ a_{\bar{n}}^+ a_l a_{\bar{l}}, \tag{2}$$

where G is a constant pairing interaction, ϵ_l are the single-particle energies, $\vec{\Omega}$ is the angular velocity, $\vec{J}$ is the total angular momentum in $\hbar$ units, λ is the Fermi energy determined for the lowest energy state, while $\hat{N} = \sum_l(a_l^+ a_l + a_{\bar{l}}^+ a_{\bar{l}})$ is the particles number operator. The sums run over the active pairing levels space. The many-body trial wave function is considered as a superposition of Bogoliubov seniority-1 and seniority-3 configurations:

$$|\varphi\rangle = \sum_i c_i a_i^+|\phi_i\rangle + \sum_i\sum_{j\neq i} c_{i,j}a_i^+\alpha_j^+\alpha_{\bar{j}}^+|\phi_i\rangle + \sum_i\sum_{j>i}\sum_{k\neq i,j} c_{i,j,k}a_i^+a_j^+a_{\bar{k}}^+|\phi_{i,j,k}\rangle. \tag{3}$$

The notations a_k^+ (or a_k) mean creation (or annihilation) single-particle operators on the single-particle state k. The conjugated time-reversed state in the level k is denoted with $\bar{k}$. The first term in the right-hand of Eq. (3) leads to excitations between seniority-1 states, the second term is responsible for virtual excitations of the seniority-1 states, while the last term leads to excitations between the seniority-1 and the seniority-3 states. In the trial wave function (3), the odd nucleons are located on the single-particle levels i, j, and k. These levels are not involved in the pairing correlations, being considered blocked. Accordingly, the structure of the active pairing levels space is modified from one configuration to another one. The modification of the BCS amplitudes from one configuration to another is called the blocking effect [53]. Being cautioned by the pairing interaction, the states $a_i^+a_j^+a_{\bar{j}}^+|\phi_{i,j,j}\rangle$ are not allowed, and should be substituted by virtual ones $a_i^+\alpha_j^+\alpha_{\bar{j}}^+|\phi_i\rangle$. The Bogoliubov wave functions are

$$\phi_i = \prod_{m\neq i}(u_{m(i)} + v_{m(i)}a_m^+a_{\bar{m}}^+), \tag{4}$$

$$\phi_{i,j,k} = \prod_{m\neq i,j,k}(u_{m(i,j,k)} + v_{m(i,j,k)}a_m^+a_{\bar{m}}^+), \tag{5}$$

where $v_{\gamma(\gamma')}$ and $u_{\gamma(\gamma')}$ are BCS amplitudes. The indexes $m(i)$ or $m(i,j,k)$ of the BCS amplitudes supply a notation for the single-particle level m of the seniority-1 or the seniority-3 configuration in which the level (i) or the levels (i,j,k) are occupied by odd nucleons, respectively. Because only the relative phase between the vacancy amplitudes and the occupation ones matters, one considers in the following that $u_{\gamma(\gamma')}$ is a real quantity and $v_{\gamma(\gamma')}$ is a complex one. To avoid double counting, the sums of the seniority-3 Bogoliubov wave functions run only for $j > i$ in Eq. (3). Moreover, a real excitation means that two nucleons should be only in time-reversal conjugate states. The virtual seniority-3 configurations are obtained within quasiparticle creation operators α_k^+ of conjugate time-reversed states. The virtual states are not influenced by the blocking effect.

The Hamiltonian is diagonal and the energies E_i of the seniority-1 states are

$$E_i = \langle a_i^+\phi_i|H-\lambda\hat{N}|a_i^+\phi_i\rangle = 2\sum_{m\neq i}|v_{m(i)}|^2(\epsilon_m-\lambda)+(\epsilon_i-\lambda)-G\left|\sum_{m\neq i}u^*_{m(i)}v_{m(i)}\right|^2-G\sum_{m\neq i}|v_{m(i)}|^4, \tag{6}$$

those of the virtual states are

$$\begin{aligned} E_{i,j} &= \langle a_i^+\alpha_j^+\alpha_{\bar{j}}^+\phi_i|H-\lambda\hat{N}|a_{i'}^+\alpha_{j'}^+\alpha_{\bar{j}'}^+\phi_{i'}\rangle \\ &= 2\sum_{m\neq i,j}|v_{m(i)}|^2(\epsilon_m-\lambda)+2u^2_{j(i)}(\epsilon_j-\lambda)+(\epsilon_i-\lambda)-G\left|\sum_{m\neq i,j}u^*_{m(i)}v_{m(i)}\right|^2-G\sum_{m\neq i,j}|v_{m(i)}|^4 \\ &\quad +G\left[u_{j(i)}v_{j(i)}\sum_{m\neq i,j}u_{m(i)}v^*_{m(i)}+u_{j(i)}v^*_{j(i)}\sum_{m\neq i,j}u_{m(i)}v_{m(i)}\right]-G|u_{j(i)}v_{j(i)}|^2-Gu^4_{j(i)}, \end{aligned} \tag{7}$$

and those of the seniority-3 states are

$$\begin{aligned} E_{i,j,k} &= \langle a_i^+a_j^+a_{\bar{k}}^+\phi_{i,j,k}|H-\lambda\hat{N}|a_{i'}^+a_{j'}^+a_{k'}^+\phi_{i',j',k'}\rangle \\ &= 2\sum_{m\neq i,j,k}|v_{m(i,j,k)}|^2(\epsilon_m-\lambda)+(\epsilon_i-\lambda)+(\epsilon_j-\lambda)+(\epsilon_k-\lambda)-G\left|\sum_{m\neq i,j,k}u^*_{m(i,j,k)}v_{m(i,j,k)}\right|^2-G\sum_{m\neq i,j,k}|v_{m(i,j,k)}|^4. \end{aligned} \tag{8}$$

In Appendix A, the components of the effective masses for the lowest energy configuration are deduced. The lowest energy configuration is the seniority-1 configuration in which the Fermi level i_F is blocked. The inertia related to another seniority-1 configuration can be deduced in a similar way by taking the corresponding blocked level as reference. The effective masses related to the shape collective coordinates q_ν and q_μ are

$$\begin{aligned} B_{\nu,\mu} &= 2\hbar^2\sum_{j\neq i_F}\sum_{k\neq j,i_F}\frac{\left(E_{i_F,j,k}-E_{i_F}\right)\left|v_{j(i_F)}u_{k(i_F)}-u_{j(i_F)}v_{k(i_F)}\right|^2\left|P_{(i_F,j,k)(i_F)}\right|^2\langle a_j^+|\frac{\partial H}{\partial q_\nu}|a_k^+\rangle\langle a_k^+|\frac{\partial H}{\partial q_\mu}|a_j^+\rangle}{\left(E_{i_F,j,k}-\sum_{m\neq i_F,j,k}T_{m(i_F,j,k)}-E_{i_F}+\sum_{m\neq i_F}T_{m(i_F)}\right)^2(\epsilon_j-\epsilon_k)^2} \\ &\quad +2\hbar^2\sum_{i'\neq i_F}\sum_{j\neq i',i_F}\frac{\left(E_{i',j}-E_{i_F}\right)\left|v_{j(i')}u_{j(i_F)}-u_{j(i')}v_{j(i_F)}\right|^2\left|P_{(i_F)(i',j)}\right|^2\langle a_{i_F}^+|\frac{\partial H}{\partial q_\nu}|a_{i'}^+\rangle\langle a_{i'}^+|\frac{\partial H}{\partial q_\mu}|a_{i_F}^+\rangle}{\left(E_{i',j}-\sum_{m\neq i',j}T_{m(i',j)}-E_{i_F}+\sum_{m\neq i_F}T_{m(i_F)}\right)^2\left(\epsilon_{i'}-\epsilon_{i_F}\right)^2} \\ &\quad +2\hbar^2\sum_{j\neq i_F}\frac{\left(E_{i_F,j}-E_{i_F}\right)\left[u_{j(i_F)}\frac{\partial v_{j(i_F)}}{\partial q_\nu}-v_{j(i_F)}\frac{\partial u_{j(i_F)}}{\partial q_\nu}\right]\left[u_{j(i_F)}\frac{\partial v^*_{j(i_F)}}{\partial q_\mu}-v^*_{j(i_F)}\frac{\partial u_{j(i_F)}}{\partial q_\mu}\right]}{\left(E_{i_F,j}-E_{i_F}\right)^2} \\ &\quad +2\hbar^2\sum_{i\neq i_F}\frac{\left(E_i-E_{i_F}\right)\left|u_{i_F(i)}u_{i(i_F)}+v^*_{i_F(i)}v_{i(iF)}\right|^2\left|P_{(i_F)(i)}\right|^2\langle a_i^+|\frac{\partial H}{\partial q_\nu}|a_{i_F}^+\rangle\langle a_{i_F}^+|\frac{\partial H}{\partial q_\mu}|a_i^+\rangle}{\left(E_i-\sum_{m\neq i}T_{m(i)}-E_{i_F}+\sum_{m\neq i_F}T_{m(i_F)}\right)^2\left(\epsilon_i-\epsilon_{i_F}\right)^2}, \end{aligned} \tag{9}$$

where the quantities

$$P_{(\gamma)(\gamma')} = \prod_{m\neq\gamma,\gamma'}\left(u_{m(\gamma)}u_{m(\gamma')}+v^*_{m(\gamma)}v_{m(\gamma')}\right) \tag{10}$$

are obtained from overlaps of the Bogoliubov functions pertaining to different configurations. The sum in the third term of the right-hand side of Eq. (9) is restricted to the active pairing levels space, where the variations of the BCS amplitudes are allowed. The other sums of the right-hand side of Eq. (9) span all the single-particle levels, excepting the blocked one, i_F, of the lowest energy seniority-1 configuration. No diagonal matrix elements are allowed. The sum over virtual states is given by the third term of the right-hand side of Eq. (9).

With $T_{\gamma(\gamma')}$ I denoted the real energy terms that are due to the variations in time of the BCS amplitudes:

$$\begin{aligned} T_{\gamma(\gamma')} &= i\hbar(u_{\gamma(\gamma')}\dot{u}_{\gamma(\gamma')}+v^*_{\gamma(\gamma')}\dot{v}_{\gamma(\gamma')}) \\ &= \frac{i\hbar}{2}(v^*_{\gamma(\gamma')}\dot{v}_{\gamma(\gamma')}-\dot{v}^*_{\gamma(\gamma')}v_{\gamma(\gamma')}) \qquad (11) \\ &= 2|v_{\gamma(\gamma')}|^2(\epsilon_\gamma-\lambda)-2G|v_{\gamma(\gamma')}|^4 \\ &\quad +\frac{1}{2}(u_{\gamma(\gamma')}v_{\gamma(\gamma')}\Delta^*_{\gamma'}+u_{\gamma(\gamma')}v^*_{\gamma(\gamma')}\Delta_{\gamma'}) \\ &\quad \times\left(\frac{v^*_{\gamma(\gamma')}v_{\gamma(\gamma')}}{u^2_{\gamma(\gamma')}}-1\right), \qquad (12) \end{aligned}$$

where $\Delta_{\gamma'} = G\sum_{\gamma''\neq\gamma'} u_{\gamma''(\gamma')}v_{\gamma''(\gamma')}$. The equality (11) is obtained by using the time derivatives of the BCS amplitudes obtained within the time-dependent pairing equations (A2) and within the condition $u^2_{\gamma(\gamma')} + |v_{\gamma(\gamma')}|^2 = 1$.

The last term in the right side of Eq. (9) is due to the presence of the odd nucleon and takes into account the mixing between seniority-1 configurations. In the denominator, the differences in energies $E_i - E_{i_F}$ are much smaller than the differences in energies $E_{i',j} - E_{i_F}$ or $E_{i_F,j,k} - E_{i_F}$ that correspond to excitations on the virtual states or on the seniority-3 configurations, respectively. Moreover, in the numerator one obtains a sum of products of BCS amplitudes, instead of a difference. Therefore, the contribution given of the last term of the Eq. (9) should be very large. In principle, one should expect that the effective mass of a odd-nucleus exceeds that of an even one.

In the trial wave function (3), the blocked levels are considered for only one component of the conjugate time reversed pair in order to avoid double counting. If the pairing is disregarded, the level i_F of the lowest energy seniority-1 configuration corresponds to the Fermi single-particle level of the system, that is, the last single-particle level occupied by the unpaired nucleon, the remaining levels of the core being filled by pairs.

The principal moments of inertia I_n for the lowest energy state i_F around the principal axis ($n = x, y, z$) are deduced in the same manner as the effective masses, being

$$
\begin{aligned}
I_n = {} & 2\sum_{j\neq i_F}\sum_{k\neq j,i_F}\frac{\left(E_{i_F,j,k}-E_{i_F}\right)\left|v_{j(i_F)}u_{k(i_F)}-u_{j(i_F)}v_{k(i_F)}\right|^2\left|P_{(i_F,j,k)(i_F)}\right|^2\langle a_j^+|J_n|a_k^+\rangle^2}{\left(E_{i_F,j,k}-\sum_{m\neq i_F,j,k}T_{m(i_F,j,k)}-E_{i_F}+\sum_{m\neq i_F}T_{m(i_F)}\right)^2}\\
& +2\sum_{i'\neq i_F}\sum_{j\neq i,i_F}\frac{\left(E_{i',j}-E_{i_F}\right)\left|v_{j(i')}u_{j(i_F)}-u_{j(i')}v_{j(i_F)}\right|^2\left|P_{(i_F)(i',j)}\right|^2\left\langle a_{i_F}^+\left|J_n\right|a_{i'}^+\right\rangle^2}{\left(E_{i',j}-\sum_{m\neq i',j}T_{m(i',j)}-E_{i_F}+\sum_{m\neq i_F}T_{m(i_F)}\right)^2}\\
& +2\sum_{i\neq i_F}\frac{\left(E_i-E_{i_F}\right)\left|u_{i_F(i)}u_{i(i_F)}+v^*_{i_F(i)}v_{i(iF)}\right|^2\left|P_{(i_F)(i)}\right|^2\left\langle a_i^+\left|J_n\right|a_{i_F}^+\right\rangle^2}{\left(E_i-\sum_{m\neq i}T_{m(i)}-E_{i_F}+\sum_{m\neq i_F}T_{m(i_F)}\right)^2}.
\end{aligned}
\tag{13}
$$

In the previous formula, the matrix elements between the states with the spin projections $\Omega = 1/2$ and $-1/2$ are not explicitly written out. The second term of the right-hand side of Eq. (13) is similar to the second term in Eq. (5-47) of Ref. [46], obtained as a second-order correction, but differs in sign. It takes into account the excitations to the virtual states of the seniority-1 configuration, with the caution that terms of the type $\langle a_i^+|O|a_i^+\alpha_j^+\alpha_{\bar{j}}^+\rangle$ (O being an operator without time derivatives) are zero. A similar expression involving three terms for the odd-nuclei moments of inertia was also given in Ref. [41].

A dynamical treatment of the inertia should include the effects due to the dissipated energy. The parameters $u_{\gamma(\gamma')}$ and $v_{\gamma(\gamma')}$ are the solutions of the time-dependent pairing equations [50,54]. These amplitudes depend on the collective velocities and are resolved for each successive deformation along the fission path [55–58]. In these circumstances, the inertia dependence versus the dissipated energy is obtained, as discussed in Ref. [48]. For low collective velocities, the BCS amplitudes follow the values of the quasistationary states. If one considers that $u_{\gamma(\gamma')}$ and $v_{\gamma(\gamma')}$ vary slowly, the terms $T_{\gamma(\gamma')}$ can be neglected and the following formulas are obtained:

$$
\begin{aligned}
B_{\nu,\mu} = {} & 2\hbar^2\sum_{j\neq i_F}\sum_{k\neq j,i_F}\frac{\left|v_{j(i_F)}u_{k(i_F)}-u_{j(i_F)}v_{k(i_F)}\right|^2\left|P_{(i_F,j,k)(i_F)}\right|^2\langle a_j^+|\frac{\partial H}{\partial q_\nu}|a_k^+\rangle\langle a_k^+|\frac{\partial H}{\partial q_\mu}|a_j^+\rangle}{\left(E_{i_F,j,k}-E_{i_F}\right)(\epsilon_j-\epsilon_k)^2}\\
& +2\hbar^2\sum_{i'\neq i_F}\sum_{j\neq i',i_F}\frac{\left|v_{j(i')}u_{j(i_F)}-u_{j(i')}v_{j(i_F)}\right|^2\left|P_{(i_F)(i')}\right|^2\left\langle a_{i_F}^+\left|\frac{\partial H}{\partial q_\nu}\right|a_{i'}^+\right\rangle\left\langle a_{i'}^+\left|\frac{\partial H}{\partial q_\mu}\right|a_{i_F}^+\right\rangle}{\left(E_{i',j}-E_{i_F}\right)\left(\epsilon_{i'}-\epsilon_{i_F}\right)^2}\\
& +2\hbar^2\sum_{j\neq i_F}\frac{\left[u_{j(i_F)}\frac{\partial v_{j(i_F)}}{\partial q_\nu}-v_{j(i_F)}\frac{\partial u_{j(i_F)}}{\partial q_\nu}\right]\left[u_{j(i_F)}\frac{\partial v^*_{j(i_F)}}{\partial q_\mu}-v^*_{j(i_F)}\frac{\partial u_{j(i_F)}}{\partial q_\mu}\right]}{\left(E_{i_F,j}-E_{i_F}\right)}\\
& +2\hbar^2\sum_{i\neq i_F}\frac{\left|u_{i_F(i)}u_{i(i_F)}+v^*_{i_F(i)}v_{i(iF)}\right|^2\left|P_{(i_F)(i)}\right|^2\langle a_i^+|\frac{\partial H}{\partial q_\nu}|a_{i_F}^+\rangle\left\langle a_{i_F}^+\left|\frac{\partial H}{\partial q_\mu}\right|a_i^+\right\rangle}{\left(E_i-E_{i_F}\right)\left(\epsilon_i-\epsilon_{i_F}\right)^2}
\end{aligned}
\tag{14}
$$

and

$$
\begin{aligned}
I_n = {} & 2\sum_{j\neq i_F}\sum_{k\neq j,i_F}\frac{\left|v_{j(i_F)}u_{k(i_F)}-u_{j(i_F)}v_{k(i_F)}\right|^2\left|P_{(i_F,j,k)(i_F)}\right|^2\langle a_j^+|J_n|a_k^+\rangle^2}{\left(E_{i_F,j,k}-E_{i_F}\right)}\\
& +2\sum_{i'\neq i_F}\sum_{j\neq i',i_F}\frac{\left|v_{j(i')}u_{j(i_F)}-u_{j(i')}v_{j(i_F)}\right|^2\left|P_{(i_F)(i',j)}\right|^2\left\langle a_{i_F}^+\left|J_n\right|a_{i'}^+\right\rangle^2}{\left(E_{i',j}-E_{i_F}\right)}+2\sum_{i\neq i_F}\frac{\left|u_{i_F(i)}u_{i(i_F)}+v^*_{i_F(i)}v_{i(iF)}\right|^2\left|P_{(i_F)(i)}\right|^2\left\langle a_i^+\left|J_n\right|a_{i_F}^+\right\rangle^2}{\left(E_i-E_{i_F}\right)}.
\end{aligned}
\tag{15}
$$

As shown in Appendix B concerning the quasistationary states, by neglecting the blocking effect one obtains

$$
\begin{aligned}
B_{\nu\mu} = {} & 2\hbar^2 \sum_{j\neq i_F} \sum_{k\neq j,i_F} \frac{(v_j u_k + u_j v_k)^2 \langle a_j^+ | \frac{\partial H}{\partial q_\nu} | a_k^+ \rangle \langle a_k^+ | \frac{\partial H}{\partial q_\nu} | a_j^+ \rangle}{(\mathcal{E}_j + \mathcal{E}_k)^3} \\
& + 2\hbar^2 \sum_{j\neq i_F} \frac{1}{8\mathcal{E}_j^5} \Bigg[\Delta^2 \frac{\partial \lambda}{\partial q_\nu} \frac{\partial \lambda}{\partial q_\mu} + (\epsilon_j - \lambda)^2 \frac{\partial \Delta}{\partial q_\nu} \frac{\partial \Delta}{\partial q_\mu} + \Delta(\epsilon_j - \lambda) \left(\frac{\partial \Delta}{\partial q_\nu} \frac{\partial \lambda}{\partial q_\mu} + \frac{\partial \lambda}{\partial q_\nu} \frac{\partial \Delta}{\partial q_\mu} \right) \\
& - \Delta^2 \left(\frac{\partial \lambda}{\partial q_\nu} \langle a_j^+ | \frac{\partial H}{\partial q_\mu} | a_j^+ \rangle + \frac{\partial \lambda}{\partial q_\mu} \langle a_j^+ | \frac{\partial H}{\partial q_\nu} | a_j^+ \rangle \right) - \Delta(\epsilon_j - \lambda) \left(\frac{\partial \Delta}{\partial q_\nu} \langle a_j^+ | \frac{\partial H}{\partial q_\mu} | a_j^+ \rangle + \frac{\partial \Delta}{\partial q_\mu} \langle a_j^+ | \frac{\partial H}{\partial q_\nu} | a_j^+ \rangle \right) \Bigg] \\
& + 2\hbar \sum_{i\neq i_F} \frac{\left(u_i u_{i_F} + v_i v_{i_F}\right)^2 \langle a_i^+ | \frac{\partial H}{\partial q_\nu} | a_{i_F}^+ \rangle \langle a_{i_F}^+ | \frac{\partial H}{\partial q_\nu} | a_i^+ \rangle}{\left(\mathcal{E}_i - \mathcal{E}_{i_F}\right)\left(\epsilon_i - \epsilon_{i_F}\right)^2}
\end{aligned}
\tag{16}
$$

for the effective masses and

$$
\begin{aligned}
I_n = {} & 2 \sum_{j\neq i_F} \sum_{k\neq j,i_F} \frac{\left(u_k v_j - v_k u_j\right)^2 \langle a_j^+ | j_n | a_k^+ \rangle^2}{\mathcal{E}_k + \mathcal{E}_j} \\
& + 2 \sum_{i\neq i_F} \frac{\left(u_i u_{i_F} + v_i v_{i_F}\right)^2 \langle a_i^+ | j_n | a_{i_F}^+ \rangle^2}{\mathcal{E}_i - \mathcal{E}_{i_F}}
\end{aligned}
\tag{17}
$$

for the moments of inertia. In Eq. (16) the sum over virtual states is translated into a sum over diagonal matrix elements. The formula (17) is almost identical to that reported in Ref. [38]. Here, $\mathcal{E}_i$ represent the quasiparticle excitation energies and Δ the pairing gap parameter. To perform the calculations for the last terms in Eqs. (16) and (17), one should consider that $v_{i_F} = 1$ if the blocking effect is disregarded, as suggested in Ref. [38]. For even nuclei, the last terms of Eqs. (16) and (17) vanish, and the classical formulas [59,60] for stationary inertia of even nuclei are retrieved. To my knowledge, an analogous formula for the collective masses for odd-nuclei has not been published so far. As an observation, only the second term in the right hand side of Eq. (16), which runs over virtual excitations, contains diagonal matrix elements of the derivatives of the Hamiltonian. This last point is not noticed in many references treating the subject. In Ref. [61], it is even considered that the sum over virtual states cannot be relevant in the calculation of the effective mass.

As anticipated previously in Sec. I, the increase of the inertia for odd-nucleon systems is due to the presence of the last terms in the right side of the above equations and to a change of the pairing gap parameter. The increase of the inertia when the pairing gap parameter decreases ca be understood in a simple way. For large values of the pairing gap parameter, the diagonal components of the mass tensor can be approximated as [60]

$$
B_{\nu,\nu} \approx \frac{\hbar^2}{16} \left| \left\langle \frac{\partial H}{\partial q_\nu} \right\rangle_{\mathrm{AV}} \right|^2 \frac{g_{\mathrm{sp}}}{\Delta^2},
\tag{18}
$$

which shows a dependence on the pairing gap parameter Δ^2 at the denominator. In the crude approximation (18), $\langle \partial H / \partial q_\nu \rangle_{\mathrm{AV}}$ represents an averaged value of the matrix elements, while g_{sp} is the level density at the Fermi energy. A smaller value of Δ is caused by the blocking effect, leading to an increase in inertia.

III. RESULTS AND DISCUSSION

The moments of inertia and the effective masses are determined along the fission path of $^{230-232}$Th nuclei in order to investigate the even-odd effect for a large amplitude motion. I use the wave functions obtained by solving the Schrödinger equation for a two-center Woods-Saxon semiphenomenological mean field. A more realistic treatment of the mean field requires the consideration of the effective interactions between nucleons as realized in the Hartree-Fock approaches [62,63]. The formalism developed in this work requires only the solutions of the eigenvalues problem, and therefore can be also applied in the case of a self-consistent approach. The mean field used in the following is managed by a nuclear shape parametrization characterized by five collective coordinates associated with different degrees of freedom of the system. These are the elongation, the necking, the mass asymmetry, and the two deformations of the fragments. The axial-symmetric nuclear shape parametrization is given by smoothly joining two aligned spheroids of different semiaxes a_i/b_i $(i = 1, 2)$ with an intermediate surface obtained by the rotation of an arc of a circle around the axis of symmetry The elongation is considered as the distance between the centers of the two spheroids and it is denoted R. The necking is given by the curvature of the arc of a circle of the intermediate region denoted C. The mass asymmetry is considered as the ratio between the major semiaxes of the two spheroids a_1/a_2, while the deformations of the fragments are given by their eccentricities ε_i. Within this nuclear shape parametrization, it is possible to describe the transition from one nucleus to two separated bodies in a continuous way. This nuclear shape parametrization was described in detail in Ref. [52], and was used to investigate the fission processes in a wide range of mass asymmetries, including α decay. A dynamical fission path is calculated to connect the ground state of the parent nucleus and the exit point of the outer barrier in accordance to the least action principle [60]. In the Wentzel-Kramers-Brillouin (WKB) approximation, this problem amounts to minimizing the classical action integral

$$
S = \frac{2}{\hbar} \int_{R_0}^{R_e} \sqrt{[V(R) - V_0] B(R)} dR,
\tag{19}
$$

where the turning points R_0 and R_e are the elongations of the ground state and of the exit point of the barrier, respectively.

Here, V_0 is the ground state energy, V is the deformation energy in the five-dimensional configurations space, while B is the effective mass along the fission trajectory:

$$B(R) = \sum_{\nu} \sum_{\mu} B_{\nu,\mu} \frac{\partial q_\nu}{\partial R} \frac{\partial q_\mu}{\partial R}. \quad (20)$$

In the previous expression, q_ν represent the generalized coordinates. In Eq. (20), the elongation R is chosen as a main generalized coordinate. The deformation energy of the nucleus is treated in the framework of the macroscopic-microscopic model [64,65]. The liquid drop part is given by the sum of several contributions: the Coulomb energy, the surface term obtained within the Yukawa-plus-exponential interaction [66], the Coulomb diffuseness correction contribution, the volume term, and the Wigner one. The precise mathematical forms of these liquid drop contributions are given in Ref. [67]. The model is extended for binary systems with different charge densities [68]. The microscopic corrections are obtained within the Strutinsky procedure [69]. The shell effects for the odd-nucleon systems are obtained in the same way as for the even ones. Namely, the smoothed Fermi energy is obtained by solving the equation for the odd number of particles. An average total energy is obtained for this smoothed value of the Fermi energy. The total energy of the system is obtained by summing twice the single-particle energies of the occupied levels located below the Fermi level and once for the single-particle energy of the last occupied level. The difference between the total energy and the averaged one gives the shell effects. For the pairing effect, the pairing gap and the Fermi energy are calculated for the same number of levels located above and below the Fermi level. The blocked level pertaining to the odd nucleon is eliminated when the BCS solutions are calculated. The number of nucleons considered in the active levels pairing space is equal to the number of levels of this space. In this work, 28 single-particle levels are taken above and below the Fermi energy as an active pairing levels space. The corresponding energy intervals depend on the deformation and are 6.01–7.97 MeV above and 6.68–8.38 MeV below the Fermi energy. In order to calculate the pairing effects, the effective strength of pairing interaction G is required. This value is calculated within a proper averaging by taking into account the energies of all single-particle states of the active levels space and an average pairing gap parameter obtained from a systematic [60]. For the same purpose, a more elaborated formalism is given in Ref. [64], in which the averaging used to obtain the pairing strength has an improved accuracy. By performing the calculations within the approach of Ref. [64], I noticed an increase of the pairing strength G of the order of 10% versus the values obtained with the theory of Ref. [60]. Also, some authors consider that the pairing strength is proportional to the surface area of the nucleus S. In this work, I work with both approaches given in Refs. [60,64] to investigate the effects of the pairing amplification on the fission barriers and on the inertia, and by postulating that $G \propto S/S_0$, S_0 being the surface area of the same nucleus considered spherical. When the pairing effects were amplified, it was observed that the theoretical fission barrier heights came close to the experimental values, as given by evaluations. The average nuclear field is obtained with the Woods-Saxon two center shell model [52], that should be more realistic than the classical Nilsson two-center shell model [70]. The Woods-Saxon mean field is modified by the Coulomb and spin-orbit interactions. Versions of two-center shell models are found in the literature [71–75]. It should be noted that other results were obtained in the framework of two-center shell models in the past to investigate the inertia. For example, cranking mass parameters were also reported in Ref. [76]. A rotating two-center shell model was investigated in Ref. [77]. In the mentioned examples, the eigenfunctions given by a semisymmetric double harmonic oscillator were used to solve a Nilsson microscopic potential.

In Ref. [48], a parametrization of the fission path in the multidimensional configuration space spanned by the five previously mentioned generalized coordinates in the case of the ^{232}Th parent nucleus was determined. The fission path originates in the ground state of the parent nucleus and arrives at the exit point of the outer barrier. The minimization of the functional (20) is very laborious. In this work, for simplicity, I renormalized this parametrization by a factor $(A/232)^{1/3}$. So, I considered that the dependencies off all the collective coordinates $q_\nu(x)$ as function of $x = (A/232)^{1/3}R$ for the nucleus A are the same as $q_\nu(R)$ for the initial nucleus ^{232}Th, for which the mass number is 232. As mentioned, R denotes the elongation of the nuclear system and it is given by the distance between the centers of the spheroids associated to the nascent fragments. In this way, the fission paths are also parametrized for the ^{230,231}Th isotopes.

The fission barriers for the low energy fission of $^{230–232}$Th are displayed in Fig. 1. The heights of the theoretical barriers are given in Table I and compared with values deduced from experimental data. The parent nuclei are indicated in the first column. Columns 2 to 4 correspond to low values of G that are obtained with the formalism of Ref. [60]; the following three columns correspond to the high values of G, given by the approach of Ref. [64], while the last columns are for evaluated data. The heights of the barriers are reported by taking as reference the energy of the ground state deformation that is renormalized with a typical zero point vibration energy of 0.5 MeV. My values agree very well with the evaluations resulting from experimental data [78]. Deviations from the empirical evaluations of the same magnitudes in the Th region are also found in the calculations given in Ref. [79], that take into account an increase of the gap parameter in the vicinity of the top of the barrier. The values of the gap parameters Δ and those of the pairing interaction G are plotted in Fig. 2 for the ^{231}Th nucleus. The pairing interactions G increase with the surface of the nucleus. The pairing gaps Δ are larger in the regions of the top of the barriers than in the ground state location. A similar behavior was also observed when a state-dependent pairing interaction was taken into consideration [80].

The experimental bandheads energies of the ^{231}Th are given by configurations of spin $5/2^+$, $5/2^-$, $3/2^+$, and $1/2^+$ at energies 0, 185.7, 221.4, and 247.6 keV, respectively [81,82]. In Fig. 3, the neutron single-particle level scheme is displayed along the fission path, the ground state being located around $R \approx 4.3$ fm. The Fermi single-particle level is marked with

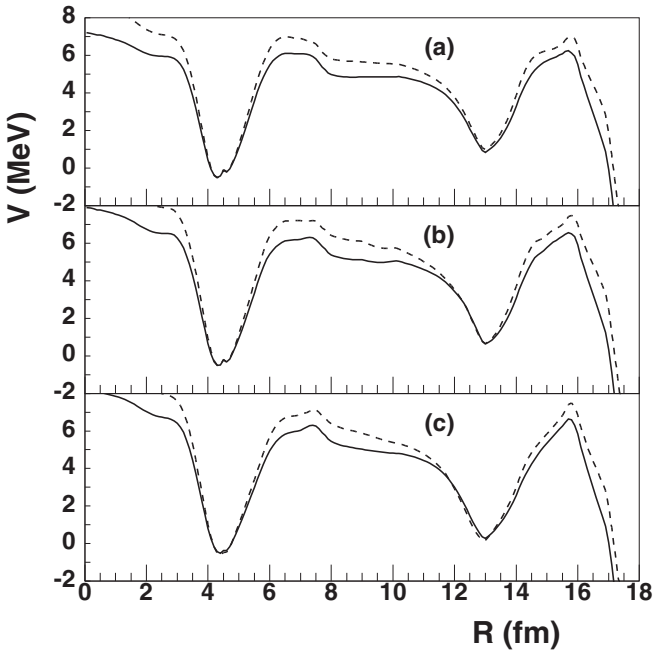

FIG. 1. The deformation energy V of the $^{230-232}$Th parent nuclei is represented as function of the distance between the centers of the spheroids associated with the nascent fragments denoted R. Panel (a) corresponds to ^{230}Th, panel (b) corresponds to ^{231}Th, and panel (c) is for ^{232}Th. The deformation energy obtained with high values of the pairing interaction G is plotted with a full line. The dashed line is used for low values of G.

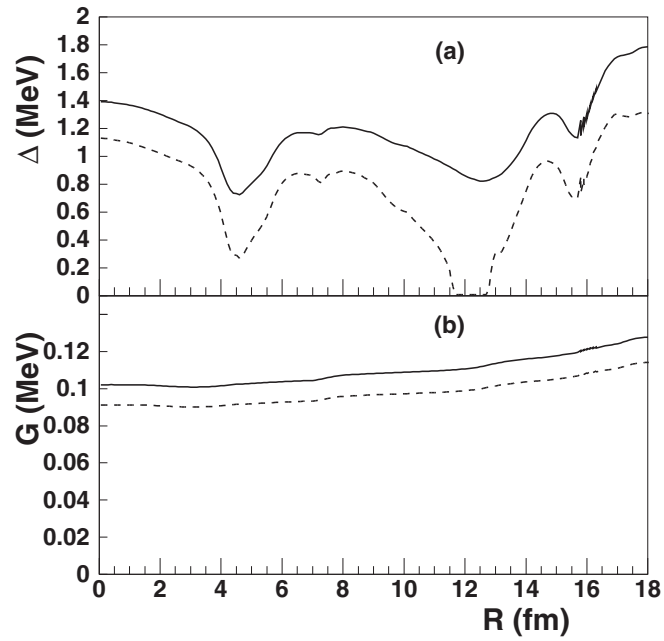

FIG. 2. The pairing gap parameters Δ and the pairing interaction G as function of the elongation R are plotted in panels (a) and (b), respectively. The full line corresponds to high values of G obtained with the formalism of [64], while the dashed line is calculated with the formalism in [60], giving low G values.

red points superimposed on the energy curves. The green, dark blue, violet, and blue curves are assigned to single-particle levels with projections of the spins $\Omega = 1/2$, $3/2$, $5/2$, and $7/2$, respectively. In the ground state, the Fermi level has $\Omega = 5/2^-$, and it is surrounded below by two levels, that is, the violet one of spin $5/2^+$ and the dark blue one of spin $3/2^+$, while above the Fermi level one obtains the green curve corresponding to spin $1/2^+$. In the single-particle representation, apart from the inversion of the levels $5/2^+$ and $5/2^-$ which are very close in energy, the experimental sequence of spins is reproduced. It is important to highlight that the density of levels around the Fermi energy is magnified in the regions of the first and second barriers. When the density of levels is increased, the probability of having crossings between single-particle levels, or avoided level crossing regions between levels with same the good quantum numbers, is much amplified. When two levels of the same spin enter in an avoided level crossing region, the radial coupling becomes very large. Also, in the case of axial-symmetric systems, when two levels that differ by one unit in their spin intersect, the matrix elements of the Coriolis coupling reach maximal values. At the same time, the difference in the quasiparticle energies of these levels approaches zero when they intersect. It can be also noted that, in the last terms in the right-hand sides of Eqs. (16) and (17), the differences in quasiparticle energies appear in the denominator and the matrix elements appear in the numerator. Therefore, in the single-particle level crossing regions, the values of moment of inertia can be extremely large if one of the two single-particle levels corresponds to the Fermi level. It is important to note that it is possible to obtain sometimes negative values of the differences in the energies of seniority-1 configurations in the level crossings. In this case I take the absolute value of the energy difference in calculations.

TABLE I. The main parameters calculated for $^{230-232}$Th potential barriers. The parent nucleus is indicated in the first column. Values for the height of the first barrier V_A, the energy of the second well V_{II} considered as a difference from the ground state energy, and the height of the second barrier V_B, are given in three sets of columns. The firsts two sets correspond to the theoretical calculations, for low values and high values of G, respectively. The superscript L indicates low values of G. The third set contains the evaluated values from experimental data [78].

Parent nucleus	V_A^L (MeV)	V_{II}^L (MeV)	V_B^L (MeV)	V_A (MeV)	V_{II} (MeV)	V_B (MeV)	$V_A^{\rm exp}$ (MeV)	$V_{II}^{\rm exp}$ (MeV)	$V_B^{\rm exp}$ (MeV)
^{230}Th	6.99	1.51	7.05	6.28	1.41	6.27	6.1		6.5
^{231}Th	7.23	1.17	7.46	6.34	1.22	6.58	6.02	<5.8	6.27
^{232}Th	7.17	0.76	7.47	6.34	0.82	6.64	5.82	<4.5	6.22

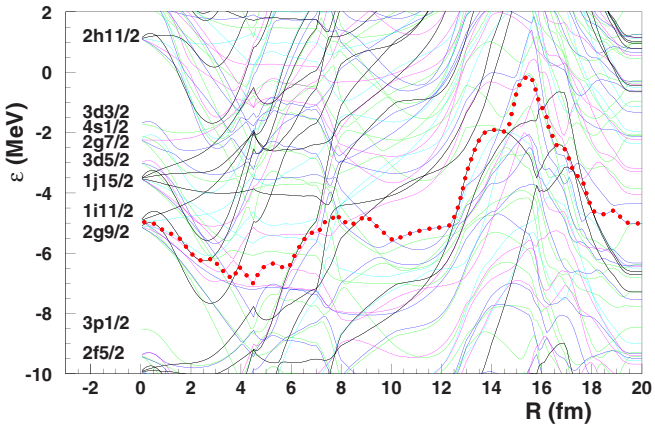

FIG. 3. The neutron single-particle level scheme ϵ in the region of the Fermi energy is represented as function of the distance between the centers of the spheroids associated with the nascent fragments R. The spherical orbitals are marked with their spectroscopic notations on the left, for $R = 0$, where a spherical nuclear shape is considered. From $R \approx 19.5$ fm, scission has occurred, and the single-particle energies remain unmodified. The ground state is located around a deformation of $R \approx 4.3$ fm. The levels with spin projection $\Omega = 1/2$ are plotted with the green curves, those with $\Omega = 3/2$ are plotted with the dark blue ones, while those with $\Omega = 5/2$ and $\Omega = 7/2$ are plotted with violet and blue, respectively. The Fermi single-particle level is identified with red points that are superimposed on the curves.

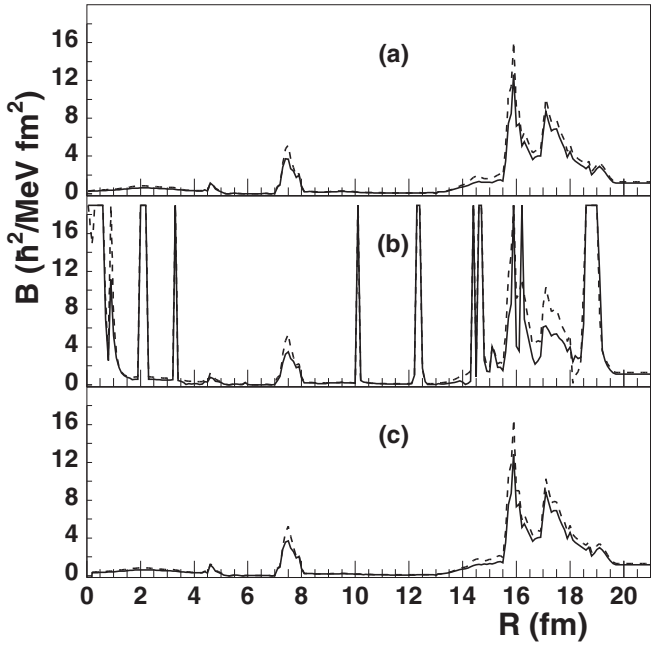

FIG. 4. The effective masses B along the fission trajectory displayed as function of the distance between the centers of the spheroids associated with the two fragments R. The parent nuclei are represented in the same order as in Fig. 1 and the meanings of the lines types are the same. In panel (b), the inertia is represented up to a maximal value of 19 $\hbar^2/(\text{MeV fm}^2)$.

The investigation of the main behavior of the inertia for odd systems is intended. For this purpose, the simplest formulas for the inertia, given by Rels. (16) and (17), are used. The effective masses B calculated with the formula (16) along the fission trajectories are represented in Fig. 4 for the $^{230-232}$Th nuclei analyzed. After scission, produced around an elongation of $R \approx 19.5$ fm, the effective masses remain constant, approaching the reduced mass. As expected, the inertia is larger almost overall for the low values of the pairing interaction G. Larger values of the inertia are obtained in the regions of the tops of the two barriers. In its path towards scission, the even-odd nuclear system exhibits abrupt variations of the collective inertia around $R = 10$, 12, 14.5, 16, and 19 fm. These fluctuations are dependent on the nuclear structure and can be explained in connection with Fig. 3, where the single-particle level scheme is displayed. For example, at $R \approx 10$ fm, two single-particle levels of the same spin projection $\Omega = 3/2$ enter an avoiding crossing region, one of them being the Fermi level. A seniority-1 configuration is assigned to each of these two single-particle levels. As previously mentioned, the quasiparticle energies associated with these two seniority-1 configurations are almost the same in the avoided level crossing region. As a consequence,the difference in the denominator of the third term in the right-hand side of Eq. (16) is very small. The matrix elements of the derivatives of the Hamiltonian are also very large between two single-particle states characterized by the same good quantum numbers. Therefore, the contribution of the radial interaction between these two states becomes huge. Around $R = 12$ fm, these two single-particle levels intersect once again. At 14.5 fm, several intersections are produced concomitantly. A blue level of spin $\Omega = 7/2$ crosses the black level of spin 9/2, but both these single-particle levels are located near an appropriate avoided crossing region. The density of single-particle levels is very high at $R = 16$ fm and the Fermi level crosses several single-particle levels. At 19 fm, an avoided level crossing region is produced between two dark blue levels of spin 3/2.

The perpendicular moment of inertia around the axis x is denoted I in the following. The variations of I as function of the elongation R for the $^{230-232}$Th nuclei are displayed in Fig. 5. The calculations are obtained within the two-center shell model formalism and by using the formula (17). As expected, again for even-even systems, the moments of inertia obtained for low values of the pairing interaction G are slightly larger than those obtained at larger values. The moment of inertia plotted for the even-odd ^{231}Th nucleus in panel (b) exhibits large fluctuations, and exceeds by appreciable amounts the values obtained for the even-even systems for some regions of the fission path.

In the ground state, the rotational parameter of ^{231}Th obtained from experimental data is 6 keV [83]. From the analysis of the fission cross section fine structure [84,85], the rotational band parameter in the region of the outer barrier, where a third minimum is postulated [86], is $\hbar^2/2I \approx 1.9-2.1$ keV. From the present theory, the values obtained in the ground state for I are 47–59, 82–82, and 48–63 $\hbar^2$/MeV for ^{230}Th, ^{231}Th, and ^{232}Th, respectively, for the the high and the low values of the pairing interaction G. These values give rotational parameters of the order of 8.5–10.6 keV for the mass $A = 230$, 6.1 keV

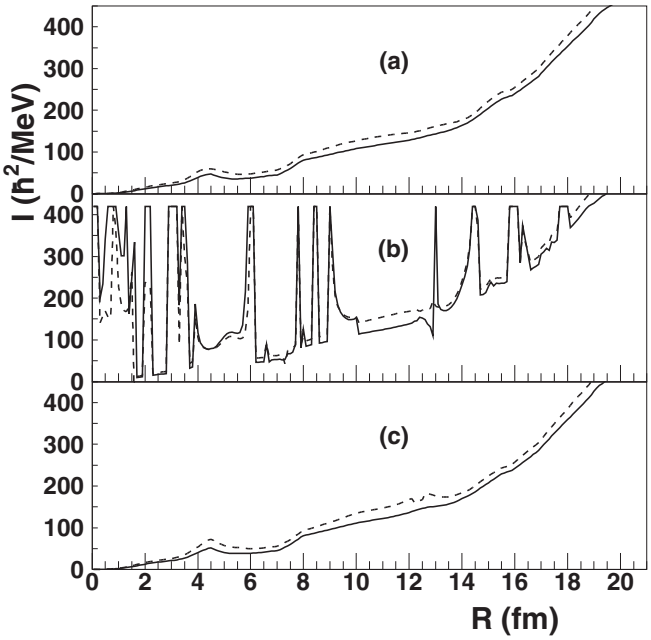

FIG. 5. The moment of inertia I perpendicular to the axis of symmetry along the fission trajectory as function of the distance between the centers of the spheroids associated with the two fragments R. The parent nuclei are represented in the same order as in Fig. 1 and the meanings of the lines types are the same. In panel (b), the moments of inertia are represented up to a maximal value of 410 $\hbar^2$/MeV.

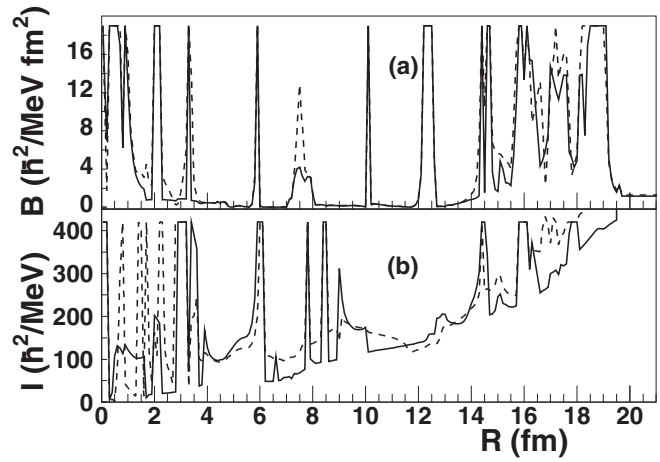

FIG. 6. The effective masses B are displayed in panel (a) and the perpendicular moments of inertia I in panel (b) as function of the distance between the centers of the spheroids associated with the two fragments R for ^{231}Th. The blocking effect is taken into account. The full curve indicates high values of the pairing interaction G while the dashed curve is for low values.

for $A = 231$, and 8–10.4 keV for $A = 232$. In the ground state of the ^{231}Th nucleus, the theoretical value of the moment of inertia agrees well with the experimental data and was not proved to be very sensitive to different values of the pairing interaction G, in the present calculations. At $R = 15.7$ fm in the case of ^{231}Th, close to the top of the second barrier, the values obtained for I are 237 and 254 $\hbar^2$/MeV for the high and, respectively, low values of G. These values can be translated in rotational parameters ranging between 2.1 and 2 keV, that are also close to those obtained for the third minimum from experimental evaluations. However, this agreement should not be considered as a proof for the existence of triple barriers, because a fine structure can be also produced by dynamical single-particle effects [87].

Just before the ground state of the parent nucleus, at $R \approx 3.7$ fm, one notices a decrease of the moment of inertia for ^{231}Th. At this elongation, as seen in Fig. 3, the Fermi level has the projection of the spin $\Omega = 9/2$. It is surrounded by $\Omega = 5/2$ levels, and other levels with spins that differ by one unit are not nearby. Therefore, for this configuration, the values of I should be small. Once the single-particle levels with $\Omega = 9/2$ and $\Omega = 5/2$ intersect, a new configuration is obtained in which the Fermi level is characterized by a projection of spin $5/2$, and has a single-particle level of spin $3/2$ in its vicinity. Between these single-particle levels that are close in energy, the Coriolis coupling contributes significantly to the value of the moment of inertia. Therefore, the values of I are magnified for this $\Omega = 5/2$ configuration. So, the values of I can vary from one seniority-1 configuration to another, according to the quantum numbers of the blocked levels. Several large fluctuations are observed for I along the fission path located at 6, 7.8, 8.5, 9, 14.5, and 16 fm. These are due mainly to crossings between levels that differ by one unit in the spin Ω. For example, at $R \approx 6$ fm, two levels of spin $\Omega = 1/2$ intersect, and the coupling between the conjugate states is very large. In another example, at $R \approx 7.8$ fm, an intersection between spin $3/2$ (dark blue) and spin $5/2$ (violet) is identified, being surrounded by many levels of spin $1/2$ and spin $7/3$.

The differences $\mathcal{E}_i - \mathcal{E}_{i_F}$ in the denominators of the last sums given the Eqs. (16) and (17) are very small in the avoided level crossing regions and when two single-particle levels of different spins intersects and produce strong fluctuations for the inertia of odd systems. Therefore, the energies of the seniority-1 configurations should be very accurately calculated. To improve the accuracy of the numerical evaluations for ^{231}Th, the collective energies were also determined within Eqs. (6)–(8) for all the states included in the active pairing levels space, by taking into account the blocking effect. The same values of the pairing interaction G were considered for all the possible configurations. Also, the formulas (14) and (15) were considered in order to calculate more precisely the inertia. The results are presented in Fig. 6. The behavior of the inertia is similar to those obtained in the previous evaluations, where the blocking effect is neglected, exhibiting a similar structure. In the ground state, the value of the moment of inertia is larger than in the case when the blocking effect is neglected, and reaches 102.3 $\hbar^2$/MeV. The two lowest energy seniority-1 configurations in the region of the ground state deformation are both assigned a spin projection $\Omega = 5/2$, and their corresponding blocked levels are close in energy. So, the structures of the active pairing levels space of the two configurations are similar around the ground state deformation. Due to the blocking effect, the BCS amplitudes are modified in such a way that the energies of the two $\Omega =$

5/2 seniority-1 configurations become almost identical, and the overlap of the collective wave functions increases, leading to larger values of the moment of inertia. It is interesting to note that in the ground state region an inversion of the values of the moment of inertia is obtained relative to the strength of the interaction G. In this region, the system possessing the higher value of G has larger values of the inertia. When G increases, the differences between the energies of the seniority-1 configurations become smaller, leading to an increase of the inertia. Overall, this increase compensates the decrease of the inertia produced for excitations to seniority-3 configurations. In the ground state, the contribution of the proton distribution is 17.1 $\hbar^2$/MeV. In the case of the neutron distribution, the successive contributions of the three terms in the right-hand side of (15) amount to 25.9, 1.1, and 58.2 $\hbar^2$/MeV. The contributions due to the second term in the right-hand side of Eqs. (14) and (15) is very small, and can be considered as a correction. The contribution of the term that takes into account seniority-1 excitations is extremely large. It can be also specified that the mean value of the overlaps $|P_{(\gamma)(\gamma')}|^2$ in the active pairing levels space is close to 1, being 0.93 for the excitations to seniority-3 configurations and 0.96 for excitations between seniority-1 configurations.

IV. CONCLUSIONS

Formulas for the moments of inertia and the mass parameters of a deforming odd-mass nuclear system are derived from the time-dependent pairing equations. The expressions obtained for the moments of inertia and the effective masses take into account the effect due to the dissipation produced during the deformation of the nuclear system. For low collective velocities, the expressions for the inertia reduce to those obtained in the framework of the superfluid cranking approximation. Similar expressions for the collective masses of odd nuclei have not been given in the literature so far in order to take into account the influence of the odd nucleon. In the formalism conceived in this work, if the blocking effect is taken into consideration it is via additional terms due to the excitations on virtual states constructed on seniority-1 configurations, that contribute to the radial or rotational inertia. For even systems, both formulations made in this work for the inertial masses and for the moments of inertia reduce to classical expressions, as also remarked in Refs. [48,49], where only even-even systems were treated. Only the inertia corresponding to the lowest energy state is derived, but the formalism can be also extended to determine the inertia relative to other configurations, by changing as a reference the configuration with blocked level i_F to another seniority-1 configuration. The behavior of the inertial parameters is investigated for the large amplitude motion of the $^{230-232}$Th isotopes. The fact that the inertia is larger when the pairing interaction is lower is confirmed. The inertia values for odd nuclear systems exhibit strong fluctuations. These are due mainly to the changes of the seniority-1 configuration considered as reference when single-particles crossings occur. In the case of ^{231}Th, the moment of inertia given by the theory agree well with those evaluated from experimental data if the blocking effect is neglected. In obtaining the results, it should be mentioned that there are some improvements in the actual calculations in comparison with the previous ones [48,49] concerning the effective masses and the moments of inertia. First of all, a pairing interaction proportional to the nuclear surface is considered. Second, the dependence of the pairing interaction as a function of the number of single-particle levels in the pairing space is obtained with a more sophisticated method, allowing an increase of its magnitude.

ACKNOWLEDGMENT

This work was supported by a grant from Ministry of Research and Innovation, CNCS-UEFISCDI, Project No. PN-III-P4-ID-PCE-2016-0092, within PNCDI III.

APPENDIX A: INERTIA FORMALISM

The calculations of the matrix elements required to perform the variation of the functional (1) are done in a way similar to that given in Ref. [48]. For example, in the case of the time derivatives, the matrix elements between seniority-1 configurations are

$$\left\langle \sum_i c_i a_i^+ \phi_i \left| -i\hbar \frac{\partial}{\partial t} \right| \sum_{i'} c_{i'} a_{i'}^+ \phi_{i'} \right\rangle = \sum_i \left[-i\hbar c_i^* \dot{c}_i - |c_i|^2 \sum_{m\neq i} T_{m(i)} \right] \delta_{ii'} - i\hbar \sum_{i,i'\neq i} c_i^* c_{i'} [u_{i'(i)}^* u_{i(i')} + v_{i'(i)}^* v_{i(i')}] \langle a_i^+ | \frac{\partial}{\partial t} | a_{i'}^+ \rangle, \quad \text{(A1)}$$

where the terms $T_{\gamma(\gamma')}$ are given by Eq. (11).

The independent variables of the functional (1) are the BCS amplitudes $u_{\gamma(\gamma')}$, $v_{\gamma(\gamma')}$ and the amplitudes c_γ of the Bogoliubov wave functions postulated in the trial function (3). Variations with respect the BCS amplitudes lead to the next equations,

$$-i\hbar \dot{v}_{\gamma(\gamma')}^* = 2v_{\gamma(\gamma')}^* (\epsilon_\gamma - \lambda) - G \sum_{\gamma''\neq\gamma} \sum_{\gamma''} \left\{ u_{\gamma''(\gamma)} v_{\gamma''(\gamma)} \left(u_{\gamma'(\gamma)} - \frac{v_{\gamma'(\gamma)} v_{\gamma'(\gamma)}}{2u_{\gamma'(\gamma)}} \right) - u_{\gamma''(\gamma)} v_{\gamma''(\gamma)} \frac{v_{\gamma'(\gamma)}^* v_{\gamma'(\gamma)}^*}{2u_{\gamma'(\gamma)}} \right\}$$
$$- 2G v_{\gamma'(\gamma)} v_{\gamma'(\gamma)}^* v_{\gamma'(\gamma)} v_{\gamma'(\gamma)}^*. \quad \text{(A2)}$$

The preceding equation can be recast in terms of single-particle densities $\rho_{\gamma(\gamma')} = |v_{\gamma(\gamma')}|^2$ and pairing moment components $\kappa_{\gamma(\gamma')} = u_{\gamma(\gamma')} v_{\gamma(\gamma')}$ yielding the well known time-dependent pairing equations [50,54], that are similar to the time-dependent Hartree-Fock-Bogoliubov equations [88–91]. These equations were also generalized to take into account the Landau-Zener effect [52], the pair-breaking mechanism [55,57], and the Coriolis coupling [58,92]. Moreover, it is also possible to fix the number of particles in the two nascent fragments [56,93] by using appropriate projections techniques in the case of fission.

The inertia emerges from the mixing of different seniority configurations through the couplings determined by the matrix elements of the time derivative and of the angular momentum operators. According to the variational principle, the derivatives with respect the independent variables c_i^* are equal to zero. That yields the equations

$$\begin{aligned}\frac{\partial\mathcal{L}}{\partial c_i^*} &= c_i E_i - i\hbar\dot{c}_i - c_i\sum_{m\neq i} T_{m(i)} - \sum_{i'\neq i} c_{i'}[u^*_{i'(i)}u_{i(i')} + v^*_{i'(i)}v_{i(i')}]\left(i\hbar\langle a_i^+|\frac{\partial}{\partial t}|a_{i'}^+\rangle + \langle a_i^+|\vec{\Omega}\vec{J}|a_{i'}^+\rangle\right)P_{(i)(i')}\\
&- i\hbar\sum_{j'\neq i} c_{i,j'}(-u^*_{j'(i)}\dot{v}^*_{j'(i)} + v^*_{j'(i)}\dot{u}_{j'(i)}) - \sum_{i'}\sum_{j'\neq i} c_{i',j'}(-u_{j'(i)}v^*_{j'(i')} + u_{j'(i')}v^*_{j'(i)})\left(i\hbar\langle a_i^+|\frac{\partial}{\partial t}|a_{i'}^+\rangle + \langle a_i^+|\vec{\Omega}\vec{J}|a_{i'}^+\rangle\right)P_{(i)(i',j')}\\
&- \sum_{j'>i}\sum_{k'\neq i,j'} c_{i,j',k'}(u_{j'(i)}v^*_{k'(i)} - v^*_{j'(i)}u_{k'(i)})\left(i\hbar\langle a_{k'}^+|\frac{\partial}{\partial t}|a_{j'}^+\rangle + \langle a_i^+|\vec{\Omega}\vec{J}|a_{i'}^+\rangle\right)P_{(i)(i,j',k')}\\
&+ \sum_{i'<i}\sum_{k'\neq i,i'} c_{i',i,k'}(u_{i'(i)}v^*_{k'(i)} - v^*_{i'(i)}u_{k'(i)})\left(i\hbar\langle a_{k'}^+|\frac{\partial}{\partial t}|a_{i'}^+\rangle + \langle a_{k'}^+|\vec{\Omega}\vec{J}|a_{i'}^+\rangle\right)P_{(i)(i',i,k')}\\
&= 0 \end{aligned} \tag{A3}$$

where the notation T_γ given by Eq. (11). The terms T_γ are used for the expressions involving the time derivative of the BCS amplitudes. Because of the antisymmetry $c_{i',i,k'} = -c_{i,i',k'}$, it follows that $+\sum_{i'<i}\sum_{k'\neq i,i'} c_{i',i,k'} = -\sum_{i'<i}\sum_{k'\neq i,i'} c_{i,i',k'}$. As a consequence, the last two terms in the right-hand side of Eq. (A3) finally give only one sum.

The same procedure applies also for the amplitudes for $c^*_{i,j}$ and $c^*_{i,j,k}$. So, two other equations are obtained:

$$\begin{aligned}\frac{\partial\mathcal{L}}{\partial c^*_{i,j}} &= c_{i,j}E_{i,j} - i\hbar\dot{c}_{i,j} + c_{i,j}\left[T^*_{j(i)} - \sum_{m\neq i,j} T_{m(i,j)}\right] - \sum_{i'} c_{i',j}[u^*_{i'(i)}u_{i(i')} - v_{i'(i)}v^*_{i(i')}]\left(i\hbar\langle a_i^+|\frac{\partial}{\partial t}|a_{i'}^+\rangle + \langle a_i^+|\vec{\Omega}\vec{J}|a_{i'}^+\rangle\right)P_{(i,j)(i',j)}\\
&- i\hbar c_i(u_{j(i)}\dot{v}_{j(i)} - v_{j(i)}\dot{u}_{j(i)}) - \sum_{i'\neq i} c_{i'}(u_{j(i)}v_{j(i')} - u_{j(i')}v_{j(i)})\left(i\hbar\langle a_i^+|\frac{\partial}{\partial t}|a_{i'}^+\rangle + \langle a_i^+|\vec{\Omega}\vec{J}|a_{i'}^+\rangle\right)P_{(i,j)(i')}\\
&= 0 \end{aligned} \tag{A4}$$

and

$$\begin{aligned}\frac{\partial\mathcal{L}}{\partial c^*_{i,j,k}} &= c_{i,j,k}E_{i,j,k} - i\hbar\dot{c}_{i,j,k} - c_{i,j,k}\sum_{m\neq i,j,k} T_{m(i,j,k)}\\
&- \sum_{i'} c_{i',j,k}[u^*_{i'(i,j,k)}u_{i(i',j,k)} + v^*_{i'(i,j,k)}v_{i(i',j,k)}]\left(i\hbar\langle a_i^+|\frac{\partial}{\partial t}|a_{i'}^+\rangle + \langle a_i^+|\vec{\Omega}\vec{J}|a_{i'}^+\rangle\right)P_{(i,j,k)(i',j,k)}\\
&- \sum_{j'} c_{i,j',k}[u^*_{j'(i,j,k)}u_{j(i,j',k)} + v^*_{j'(i,j,k)}v_{j(i,j',k)}]\left(i\hbar\langle a_j^+|\frac{\partial}{\partial t}|a_{j'}^+\rangle + \langle a_j^+|\vec{\Omega}\vec{J}|a_{j'}^+\rangle\right)P(i,j,k)(i,j',k)\\
&- \sum_{k'} c_{i,j,k'}[u^*_{k'(i,j,k)}u_{k(i,j,k')} + v^*_{k'(i,j,k)}v_{k(i,j,k')}]\left(i\hbar\langle a_k^+|\frac{\partial}{\partial t}|a_{k'}^+\rangle + \langle a_k^+|\vec{\Omega}\vec{J}|a_{k'}^+\rangle\right)P(i,j,k)(i,j,k')\\
&+ \begin{Bmatrix}(-c_i)(u_{j(i)}v_{k(i)} - v_{j(i)}u_{k(i)})\left(i\hbar\langle a_j^+|\frac{\partial}{\partial t}|a_k^+\rangle + \langle a_j^+|\vec{\Omega}\vec{J}|a_k^+\rangle\right)P_{(i,j,k)(i)}\delta_{ii'}, & \text{for } j>i\\ +c_j(u_{i(j)}v_{k(i)} - v_{i(j)}u_{k(j)})\left(i\hbar\langle a_i^+|\frac{\partial}{\partial t}|a_k^+\rangle + \langle a_i^+|\vec{\Omega}\vec{J}|a_k^+\rangle\right)P_{(i,j,k)(j)}\delta_{ji'}, & \text{for } j<i\end{Bmatrix}\\
&= 0. \end{aligned} \tag{A5}$$

For a quasiadiabatic motion, one assumes that the system is in its lowest energy seniority-1 state denoted i_F. Accordingly, the amplitudes of the trial wave functions are $c_{i_F} = 1$, $c_{i\neq i_F} = 0$, $c_{i,j} = 0$, and $c_{i,j,k} = 0$. Within these assumptions, solutions of Eqs. (A3)–(A5) are obtained in a simple way. The case c_i, for $i \neq i_F$, is worked out as an example. By considering that the nucleus is in its lowest energy state, the equations for the mixing of seniority-1 configurations are obtained from Eq. (A3) as

$$\dot{c}_i + \frac{i}{\hbar}c_i\left[E_i - \sum_{m\neq i} T_{m(i)}\right] + \frac{i}{\hbar}c_{i_F}\left[u_{i_F(i)}u_{i(i_F)} + v^*_{i_F(i)}v_{i(i_F)}\right]\left(i\hbar\langle a_i^+|\frac{\partial}{\partial t}|a_{i_F}^+\rangle + \langle a_i^+|\vec{\Omega}\vec{J}|a_{i_F}^+\rangle\right)P_{(i_F)(i)} = 0. \tag{A6}$$

This kind of equation can be solved using the method of variation of constants. The previous equation is put in the form

$$\frac{\partial c_i}{\partial t} + Pc_i = Q, \tag{A7}$$

where

$$P = \frac{i}{\hbar}\left(E_i + \sum_{m\neq i} T_{m(i)}\right) \tag{A8}$$

and

$$Q = -\frac{i}{\hbar} c_{i_F}\left[u_{i_F(i)}u_{i(i_F)} + v^*_{i'(i)}v_{i(i')}\right]\left(i\hbar\langle a_i^+|\frac{\partial}{\partial t}|a_{i_F}^+\rangle + \langle a_i^+|\vec{\Omega}\vec{J}|a_{i_F}^+\rangle\right)P_{(i_F)(i)}. \tag{A9}$$

The homogeneous solution is

$$c_i^H = C_1 \exp\left(-\int P dx\right) = C_1 \exp\left[-\frac{i}{\hbar}\int_0^t \left(E_i - \sum_{m\neq i} T_{m(i)}\right)\mathrm{d}t\right], \tag{A10}$$

and the general solution is

$$\begin{aligned} c_i &= C_1\left[\int Q\exp\left(\int P dt\right)dt + C_2\right]\exp\left(\int -P dt\right) \\ &= C_1\Bigg\{-\frac{i}{\hbar}\int c_{i_F}^H\left[u_{i_F(i)}u_{i(i_F)} + v^*_{i_F(i)}v_{i(i_F)}\right]\left(i\hbar\langle a_i^+|\frac{\partial}{\partial t}|a_{i_F}^+\rangle + \langle a_i^+|\vec{\Omega}\vec{J}|a_{i_F}^+\rangle\right)P_{(i_F)(i)} \\ &\quad\times\exp\left[\int\frac{i}{\hbar}\left(E_i - \sum_{m\neq i}T_{m(i)}\right)dt\right]dt + C_2\Bigg\}\exp\left[\int -\frac{i}{\hbar}\left(E_i - \sum_{m\neq i}T_{m(i)}\right)dt\right], \end{aligned} \tag{A11}$$

C_1, C_2 being constants. In the above equation, I denoted the homogeneous solution for the seniority-1 state with $c_{i_F}^H$. Therefore, I obtain by setting the constants $C_2 = 0$ and $C_1 = 1$

$$\begin{aligned} c_i &= -\frac{i}{\hbar}\int\left[u_{i_F(i)}u_{i(i_F)} + v^*_{i_F(i)}v_{i(i_F)}\right]\left(i\hbar\langle a_i^+|\frac{\partial}{\partial t}|a_{i_F}^+\rangle + \langle a_i^+|\vec{\Omega}\vec{J}|a_{i_F}^+\rangle\right)P_{(i_F)(i)} \\ &\quad\times\exp\left[\int\frac{i}{\hbar}\left(E_i - E_{i_F} - \sum_{m\neq i}T_{m(i)} + \sum_{m\neq i_F}T_{m(i_F)}\right)dt\right]dt\exp\left[\int -\frac{i}{\hbar}\left(E_i - \sum_{m\neq i}T_{m(i)}\right)dt\right] \\ &= -\frac{\left[u_{i_F(i)}u_{i(i_F)} + v^*_{i_F(i)}v_{i(i_F)}\right]\left(i\hbar\langle a_i^+|\frac{\partial}{\partial t}|a_{i_F}^+\rangle + \langle a_i^+|\vec{\Omega}\vec{J}|a_{i_F}^+\rangle\right)P_{(i_F)(i)}}{E_i - E_{i_F} - \sum_{m\neq i}T_{m(i)} + \sum_{m\neq i_F}T_{m(i_F)}}c_{i_F}^H. \end{aligned} \tag{A12}$$

The same procedure is repeated for the seniority-3 and virtual states. By assuming that the nuclear system is in the lower energy state $c_{i_F}^H = 1$, four solutions are obtained: c_i for the seniority-1 real states, $c_{i_F,j}$ and $c_{i',j}$ for the virtual seniority-3 states, and $c_{i_F,j,k}$ for the seniority-3 real states.

Now the amplitudes obtained for the different configurations should be related to the variation of the collective kinetic energy. To make the problem tractable, first of all the derivatives of the Hamiltonian instead of the time derivatives are involved:

$$\langle a_i^+|\frac{\partial}{\partial t}|a_{i'}^+\rangle = \frac{\langle a_i^+|\frac{\partial H}{\partial t}|a_{i'}^+\rangle}{\epsilon_i - \epsilon_{i'}}. \tag{A13}$$

The derivative with respect to time is substituted by the partial derivatives with respect to the collective coordinates q_ν ($\nu = 1, N$).

$$\langle a_i^+|\frac{\partial H}{\partial t}|a_{i'}^+\rangle = \sum_\nu\langle a_i^+|\frac{\partial H}{\partial q_\nu}|a_{i'}^+\rangle\dot{q}_\nu. \tag{A14}$$

By preserving the total energy of the nuclear system, the moments of inertia and the effective masses emerge. The collective excitations are translated in variations of the collective velocities and of the collective rotations

$$\sum_{\nu,\mu}\frac{1}{2}B_{\nu,\mu}\dot{q}_\nu\dot{q}_\mu+\sum_n\frac{1}{2}\Omega_n^2I_n^2=\sum_{i\neq i_F}|c_i|^2\left(E_i-E_{i_F}\right)+\sum_{j\neq i_F}\left|c_{i_F,j}\right|^2\left(E_{i_F,j}-E_{i_F}\right)+\sum_{i\neq i_F}\sum_{j\neq i,i_F}|c_{i,j}|^2\left(E_{i,j}-E_{i_F}\right)$$
$$+\sum_{j\neq i_F}\sum_{k\neq j,i_F}\left|c_{i_F,j,k}\right|^2\left(E_{i_F,j,k}-E_{i_F}\right), \tag{A15}$$

where I_n are principal moments of inertia about the axis $n=x,y,z$.

By identifying the terms proportional to the collective velocities $\dot{q}_\nu\dot{q}_\mu$ and the collective frequencies Ω_i^2, the collective inertia are obtained as given by formulas (9) and (13), eventually.

APPENDIX B: QUASISTATIONARY STATES WITHOUT BLOCKING

By neglecting the blocking effect, the second terms in the right-hand sides of Eqs. (14) and (15) vanish because $v_{j(i_F)}u_{j(i_F)}-u_{j(i_F)}v_{j(i_F)}=0$. The overlaps $P_{(\gamma)(\gamma)}$ become unity. For stationary states, the BCS amplitudes are real numbers:

$$v_m^2=\frac{1}{2}\left(1-\frac{\epsilon_m-\lambda}{\mathcal{E}_m}\right),\quad u_m^2=\frac{1}{2}\left(1+\frac{\epsilon_m-\lambda}{\mathcal{E}_m}\right), \tag{B1}$$

where $\mathcal{E}_m=\sqrt{(\epsilon_m-\lambda)^2+\Delta^2}$ are quasiparticle energies.

The excitations are given in terms of quasiparticle energies,

$$E_{i_F,j,k}-E_{i_F}=\mathcal{E}_j+\mathcal{E}_k;\quad E_i-E_{i_F}=\mathcal{E}_i-\mathcal{E}_{i_F}. \tag{B2}$$

In the BCS theory, the relation

$$\left(\frac{v_mu_n-u_mv_n}{\epsilon_m-\epsilon_n}\right)^2=\left(\frac{v_mu_n+u_mv_n}{\mathcal{E}_m+\mathcal{E}_n}\right)^2 \tag{B3}$$

holds and the first term of the right-hand side of Eq. (14) is transformed.

Concerning the third term of Eq. (14), one needs the following identities derived from the BCS equations:

$$\frac{\partial u_m^2}{\partial q_\nu}=2u_m\frac{\partial u_m}{\partial q_\nu}=-2v_m\frac{\partial v_m}{\partial q_\nu}$$
$$=\frac{\Delta}{2\mathcal{E}_m^3}\left[\Delta\left(\frac{\partial\epsilon_m}{\partial q_\nu}-\frac{\partial\lambda}{\partial q_\nu}\right)-(\epsilon_m-\lambda)\frac{\partial\Delta}{\partial q_\nu}\right], \tag{B4}$$

$$\langle a_i^+|\frac{\partial H}{\partial q_\nu}|a_i^+\rangle=\frac{\partial\epsilon_i}{\partial q_\nu}, \tag{B5}$$

and

$$(u_mv_m)^2=\frac{1}{4}\frac{\Delta^2}{\mathcal{E}_m^2}. \tag{B6}$$

Within the previous identities and after some obvious calculations, the third term in the right-hand side of Eq. (14) becomes the second term of the Eq. (16).

[1] D. R. Inglis, Phys. Rev. **96**, 1059 (1954).
[2] D. R. Inglis, Phys. Rev. **103**, 1786 (1956).
[3] A. Bohr and B. Mottelson, Dan. Mat. Fys. Medd. **30**, 1 (1955).
[4] H. J. Lipkin, A. de-Shalit, and J. Talmi, Phys. Rev. **103**, 1773 (1956).
[5] D. J. Thouless and J. G. Valatin, Nucl. Phys. **31**, 211 (1962).
[6] G. Schutte, Z. Phys. A **283**, 183 (1977).
[7] J. Kunz and J. R. Nix, Z. Phys. A **321**, 455 (1985).
[8] S. Liran, H. J. Scheefer, W. Scheid, and W. Greiner, Nucl. Phys. A **248**, 191 (1975).
[9] A. Iwamoto and J. A. Maruhn, Z. Phys. A **293**, 315 (1979).
[10] K. Pomorski and H. Hofmann, Phys. Lett. B **263**, 164 (1991).
[11] A. S. Umar, V. E. Oberacker, and C. Simenel, Phys. Rev. C **92**, 024621 (2015).
[12] Y. Alhassid, G. F. Bertsch, L. Fang, and S. Liu, Phys. Rev. C **72**, 064326 (2005).
[13] S. T. Belyaev, Mat. Fys. Medd. Dan. Vid. Selsk. **31**, 11 (1959).
[14] A. B. Migdal, Nucl. Phys. **13**, 655 (1959).
[15] J. J. Griffin and M. Rich, Phys. Rev. **118**, 850 (1960).
[16] S. G. Nilsson and O. Prior, Mat. Fys. Medd. Dan. Vid. Selsk. **32**, 16 (1961).
[17] J. P. Davidson, Rev. Mod. Phys. **37**, 105 (1965).
[18] F. S. Stephens, Rev. Mod. Phys. **47**, 43 (1975).
[19] A. Sobiczewski, S. Bjornholm, and K. Pomorski, Nucl. Phys. A **202**, 274 (1973).
[20] K. Pomorski, B. Nerlo-Pomorska, I. Ragnarsson, R. K. Sheline, and A. Sobicewski, Nucl. Phys. A **205**, 433 (1973).
[21] R. A. Sorensen, Rev. Mod. Phys. **45**, 353 (1973).
[22] M. Brack, T. Ledergerber, and H. C. Pauli, Nucl. Phys. A **234**, 185 (1974).
[23] N. H. Allal and M. Fellah, Phys. Rev. C **43**, 2648 (1991).
[24] W. Satula and R. A. Wiss, Rep. Prog. Phys. **68**, 131 (2005).
[25] I. Ami, M. Fellah, and N. H. Allal, Rom. J. Phys. **60**, 1420 (2015).
[26] M. J. A. de Voigt, J. Dudek, and Z. Szymanski, Rev. Mod. Phys. **55**, 949 (1983).
[27] A. Bulgac, A. Klein, N. R. Walet, and G. Do Dang, Phys. Rev. C **40**, 945 (1989).
[28] M. Hasegawa and S. Tazaki, Phys. Rev. C **47**, 188 (1993).
[29] E. K. Yuldashbaeva, J. Libert, and, P. Quentin, Phys. Lett. B **461**, 1 (1999).
[30] J. Sadhukhan, K. Mazurek, A. Baran, J. Dobaczewski, W. Nazarewicz, and J. A. Sheikh, Phys. Rev. C **88**, 064314 (2013).
[31] J. Sadhukhan, J. Dobaczewski, W. Nazarewicz, J. A. Sheikh, and A. Baran, Phys. Rev. C **90**, 061304(R) (2014).

[32] H. Goutte, J. F. Berger, P. Casoli, and D. Gogny, Phys. Rev. C **71**, 024316 (2005).
[33] C. Simenel, Eur. Phys. J. A **48**, 152 (2012).
[34] R. Bernard, H. Goutte, D. Gogny, and W. Younes, Phys. Rev. C **84**, 044308 (2011).
[35] Z. P. Li, T. Niksic, P. Ring, D. Vretenar, J. M. Yao, and J. Meng, Phys. Rev. C **86**, 034334 (2012).
[36] J. Zhao, B.-N. Lu, T. Niksic, D. Vretenar, and S.-G. Zhou, Phys. Rev. C **93**, 044315 (2016).
[37] Yu. T. Grin', S. I. Drozdov, and D. F. Zaretskii, J. Expt. Theor. Phys. (U.S.S.R.) **38**, 1297 (1960) [Sov. Phys. JETP **11**, 936 (1960)].
[38] O. Prior, F. Boehm, and S. G. Nilsson, Nucl. Phys. A **110**, 257 (1968).
[39] I. Hamamoto and T. Udagawa, Nucl. Phys. A **126**, 241 (1969).
[40] P. Ring, H. J. Mang, and B. Banerjee, Nucl. Phys. A **225**, 141 (1974).
[41] M. Iwasaki and M. Yamamura, Prog. Theor. Phys. **55**, 1798 (1976).
[42] J. Y. Zeng, T. H. Jin, and Z. J. Zhao, Phys. Rev. C **50**, 1388 (1994).
[43] Y. Ando, S. Tazaki, and M. Hasegawa, Phys. Rev. C **58**, 3286 (1998).
[44] F. R. Xu, R. Wyss, and P. M. Walker, Phys. Rev. C **60**, 051301(R) (1999).
[45] S. G. Zhou, C. K. Zheng, and J. M. Hu, Phys. Rev. C **63**, 047305 (2001).
[46] A. Bohr and B. R. Mottelson, *Nuclear Structure Volume II: Nuclear Deformations* (World Scientific, Singapore, 1998).
[47] Y. Sun, C.-L. Wu, D. H. Feng, J. L. Egido, and M. Guidry, Phys. Rev. C **53**, 2227 (1996).
[48] M. Mirea, J. Phys. G **43**, 105103 (2016).
[49] M. Mirea and R. C. Bobulescu, J. Phys. G **37**, 055106 (2010).
[50] S. E. Koonin and J. R. Nix, Phys. Rev. C **13**, 209 (1976).
[51] M. Mirea and A. Sandulescu, Rom. Rep. Phys. **70**, 201 (2018).
[52] M. Mirea, Phys. Rev. C **78**, 044618 (2008).
[53] P. Ring and P. Schuck, *The Nuclear Many Body Problem* (Springer-Verlag, New York, 1980).
[54] J. Blocki and H. Flocard, Nucl. Phys. A **273**, 45 (1976).
[55] M. Mirea, Phys. Lett. B **680**, 316 (2009).
[56] M. Mirea, Phys. Rev. C **83**, 054608 (2011).
[57] M. Mirea, Phys. Rev. C **89**, 034623 (2014).
[58] M. Mirea, Phys. Rev. C **96**, 064607 (2017).
[59] T. Ledergerber and H.-C. Pauli, Nucl. Phys. A **207**, 1 (1973).
[60] M. Brack, J. Damgaard, A. S. Jensen, H. C. Pauli, V. M. Strutinsky, and C. Y. Wong, Rev. Mod. Phys. **44**, 320 (1972).
[61] B. Mohammed-Azizi, Electron. J. Theor. Phys. **9**, 143 (2012).
[62] N. Schunck and L. M. Robledo, Rep. Prog. Phys. **79**, 116301 (2016).
[63] W. Younes, D. M. Gogny, and J.-F. Berger, *A Microscopic Theory of Fission Dynamics Based on the Generator Coordinate Method*, Lectures Notes in Physics Vol. 950 (Springer, Cham, 2019).
[64] J. R. Nix, Annu. Rev. Nucl. Sci. **22**, 65 (1972).
[65] H. C. Pauli, Phys. Rep. **7**, 35 (1973).
[66] K. T. R. Davies and J. R. Nix, Phys. Rev. C **14**, 1977 (1976).
[67] P. Moller, J. R. Nix, W. D. Myer, and W. J. Swiatecki, At. Data. Nucl. Data. Tables **59**, 185 (1995).
[68] M. Mirea, O. Bajeat, F. Clapier, F. Ibrahim, A. C. Mueller, N. Pauwels, and J. Proust, Eur. Phys. J. A **11**, 59 (2001).
[69] V. M. Strutinsky, Nucl. Phys. A **95**, 420 (1967).
[70] J. A. Maruhn and W. Greiner, Z. Phys. **251**, 431 (1972).
[71] A. Diaz-Torres and W. Scheid, Nucl. Phys. A **757**, 373 (2005).
[72] A. Diaz-Torres, Phys. Rev. Lett. **101**, 122501 (2008).
[73] A. Diaz-Torres, Comput. Phys. Commun. **224**, 381 (2018).
[74] V. O. Nesterov, Nucl. Phys. A **974**, 124 (2018).
[75] N. Roshanbakht and M. R. Shojaei, Adv. High Energy Phys. **2017**, 9309636 (2017).
[76] V. Schneider, J. Maruhn, and W. Greiner, Z. Phys. A **323**, 111 (1986).
[77] X. Wu, J. A. Maruhn, and W. Greiner, Z. Phys. A **334**, 207 (1989).
[78] S. Bjornholm and J. E. Lynn, Rev. Mod. Phys. **52**, 725 (1980).
[79] K.-H. Schmidt and B. Jurado, Rep. Prog. Phys. **81**, 106301 (2018).
[80] M. Mirea, Int. J. Mod. Phys. E **27**, 1850076 (2018).
[81] D. H. White, H. G. Borner, R. W. Hoff, K. Schreckenbach, W. F. Davidson, T. von Egidy, D. D. Warner, P. Jeuch, G. B. Barreau, W. R. Kane, M. L. Stelts, R. E. Chrien, R. F. Casten, R. G. Lanier, R. W. Lougheed, R. T. Kouzes, R. A. Naumann, and R. Dewberry, Phys. Rev. C **35**, 81 (1987).
[82] E. Browne and J. K. Tuli, Nucl. Data Sheets **114**, 751 (2013).
[83] K. Jain and A. K. Jain, At. Data Nucl. Data Tables **50**, 269 (1992).
[84] J. Blons, C. Mazur, D. Paya, M. Ribrag, and H. Weigmann, Phys. Rev. Lett. **41**, 1282 (1978).
[85] J. Blons, Nucl. Phys. A **502**, 121 (1989).
[86] P. Moller, Nucl. Phys. A **192**, 529 (1972).
[87] M. Mirea, L. Tassan-Got, C. Stephan, C. O. Bacri, and R. C. Bobulescu, Europhys. Lett. **73**, 705 (2006).
[88] B. Avez, C. Simenel, and Ph. Chomaz, Phys. Rev. C **78**, 044318 (2008).
[89] S. Ebata, T. Nakatsukasa, T. Inakura, K. Yoshida, Y. Hashimoto, and K. Yabana, Phys. Rev. C **82**, 034306 (2010).
[90] G. Scamps, C. Simenel, and D. Lacroix, Phys. Rev. C **92**, 011602(R) (2015).
[91] Y. Tanimura, D. Lacroix, and G. Scamps, Phys. Rev. C **92**, 034601 (2015).
[92] M. Mirea, Europhys. Lett. **124**, 12001 (2018).
[93] M. Mirea, Phys. Lett. B **717**, 252 (2012).